Proceedings of the 2003 IEEE International Frequency Control Symposium and PDA Exhibition
Jointly with the 17th European Frequency and Time Forum

AN OSCILLATOR FOR SPACE

S. GALLIOU[1], M. MOUREY[1], F. MARIONNET[1], R. J. BESSON[1] and P. GUILLEMOT[2]

[1]Laboratoire de Chronométrie Electronique et Piézoélectricité, ENSMM
26 Chemin de l'Epitaphe 25030 Besançon Cedex, France.

[2]Centre National d'Études Spatiales (CNES)
18 avenue Édouard Belin, 31401 Toulouse Cedex 9, France.

Abstract - **These last years a new 10 MHz Quartz Crystal Oscillator family has been designed in LCEP with the support of the French space agency (CNES). It is intended for space applications especially. In this paper, the description of its general features is followed by two parts.**

The first one described the methodology which has been developed for designing such an oscillator. This part deals with the modeling of noise as well as the mechanical and thermal structure of the oscillator.

The second part summarizes main experimental results. This obviously includes the frequency stability of the oscillator and its behavior when various disturbances occur in its environment. We particularly took care of its sensitivity to external temperature changes at the atmospheric pressure and mainly under vacuum. Exhibited frequency sensitivities to a magnetic field and vibrations are also provided.

Keywords **– Quartz crystal oscillator, space applications**

I. INTRODUCTION

Very good noise results were obtained with 10 MHz SC cut BVA resonators in 1998, 1999 [1]. These resonators were selected units among usual resonator batches from the laboratory. However, their associated oscillators were not designed for space. This is why oscillators which are described below were originally designed to exhibit the best results in terms of frequency stability when operating in space environment.

Then, specific batches of BVA resonators have been dedicated for these quartz crystal oscillators for space. The overall mechanical structure of these oscillators has been completely designed in order to be as less sensitive as possible to vibrations, external temperature changes, magnetic field and radiations.

The presented results show the actual test conditions initially defined for such an oscillator environment.

II. GENERAL DESCRIPTION

The outside look of this new space oscillator is a 70 mm long, 65 mm large, 53 mm high duralumin box (see Fig. 1-a). At the present time, its mass is 425g but it could be made lighter by scooping out the present massive external enclosure.

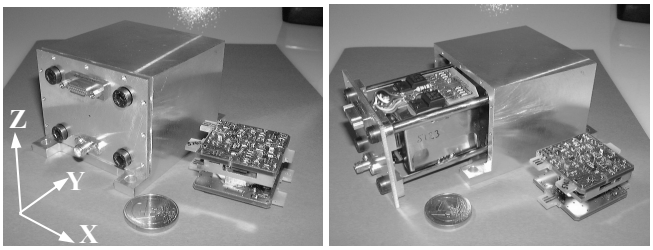

(a) (b)

Fig. 1. Space oscillator (a) Outside view (b) When it is opened.

With a general power supply of 15 V, the warm up consumption is typically set at 500 mA, whereas at an ambient temperature of 300 K, it falls down at 200 mA in steady state in still air at the atmospheric pressure and at 60 mA under vacuum.

The output provides a 6 dBm sine voltage at 10 MHz,.with an output impedance of 50 Ω. Moreover, the output frequency can be adjusted within -2 Hz, +1.5 Hz around its nominal value.

The heart of this oscillator is a 10 MHz, 3rd overtone SC cut BVA resonator surrounded with its temperature-controlled oven. Both the oscillator and thermal regulator printed circuit boards are put on each side of the resonator oven. This heart has been isolated from the oscillator body in Fig. 1-a and 1-b. It is designed to be positioned into mumetal shells which are sustained into the duralumin enclosure by four supports, as shown in Fig. 1-b. These supports have a double role. First, obviously, a mechanical one. Second, they are the main thermal path between the heart and the outer enclosure of the structure. Indeed, thermal insulating foam is prohibited for space applications.

III. DESIGN PROCESSES

A. Electronics

Electronics design is based on experience and know-how, helped with CAD tools such as SPICE. The described devices are equipped with an oscillator electronic design which gave very good results before ($\sigma(\tau) = 5\ 10^{-14}$ for 1 s < τ < 5 s) [1].

The oscillator design process can be divided in four operations, as follows:

1) *Circuit design and calculus*.

2) *SPICE simulation of the open loop oscillator*: it consists of a small signal analysis (AC analysis in SPICE) where a frequency sweep with very small steps is performed. This is possible with the actual quality factor of the resonator. The open-loop load must be taken into account. It can be simulated by reproducing the open loop circuit at least 3 times (see. Fig. 2.). Results of this step are first, the adjustments of gain and phase in order to get the oscillating conditions for which $G(\nu_c) \times H(\nu_c) = 1$ where G and H are the amplifier and the band-pass filter transfer functions respectively and ν_c the oscillator frequency, second, the exact oscillating frequency $\nu_c = \nu_{QXR} + \Delta\nu$, where ν_{QXR} is the resonant frequency of the Quartz Crystal Resonator (QXR). $\Delta\nu$ depends on the amplifier structure. Typically $\Delta\nu$ is about 10 Hz.

3) *SPICE simulation of the closed loop oscillator:* Transient analysis can be performed provided that the resonator Q factor is divided by at least 10. This step gives a look of signals when non linearities operate. This analysis includes optimization of signal levels, output amplifier, harmonics rate, output impedance…

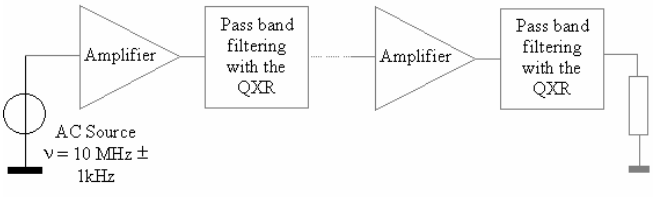

Fig. 2. Open loop analysis. The open loop oscillator must be reproduced at least one time against between its input and output copies.

4) *Noise simulation*: it is developed from SPICE results with SPICE or analytically. A closed loop, which is able to oscillate in our case, looks like Fig. 3. In this figure, $\bar{g}(t)$ and $\bar{h}(t)$ denote the "normalized" impulse responses of the amplifier and filter, respectively. Their Fourier transforms are:

$$\bar{G}(\nu) = \frac{G(\nu)}{G(\nu_c)} \text{ and } \bar{H}(\nu) = \frac{H(\nu)}{H(\nu_c)}$$

where ν_c is the carrier frequency here equal to the oscillator frequency ($G(\nu_c)\cdot H(\nu_c) = 1$ in steady state). Indeed, phase noise is relative to the carrier power. Thus, it is convenient to define this normalized set of functions [2].

It is easy to show that the Power Spectral Density (PSD) $S_{\varphi i}^{OL}$ of phase fluctuations $\varphi_i(t)$ at point I when the loop is opened is:

$$S_{\varphi i}^{OL}(\nu) = \left|\bar{G}(\nu)\right|^2 \cdot S_{nh}(\nu) + S_{ng}(\nu) \qquad (1)$$

where $S_{nh}(\nu)$ and $S_{ng}(\nu)$ are the filter caused noise and amplifier caused noise PSDs respectively.

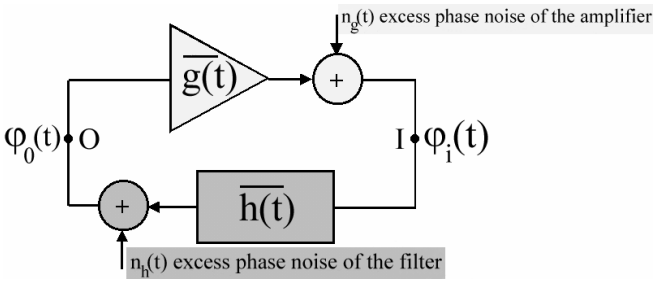

Fig. 3. Resulting closed loop circuit.

When closing the open loop the PSD of phase fluctuations $S_{\varphi i}^{CL}$ of $\varphi_i(t)$ can be expressed in terms of PSDs of both noises $n_h(t)$ and $n_g(t)$ [2][3]:

$$S_{\varphi i}^{CL}(\nu) = \frac{1}{\left|\bar{G}\cdot\bar{H}(\nu) - 1\right|^2} \cdot \left[\ \left|\bar{G}(\nu)\right|^2 \cdot S_{nh}(\nu) + S_{ng}(\nu)\ \right] \qquad (2)$$

That is to say:

$$S_{\varphi i}^{CL}(\nu) = \frac{1}{\left|\bar{G}\cdot\bar{H}(\nu) - 1\right|^2} \cdot S_{\varphi i}^{OL}(\nu) \qquad (3)$$

These PSDs are usually expressed in dBc/Hz

B. Thermo-mechanical structure

A finite element method has been used for the mechanical aspect. We chose to reject the natural modes of vibration of the structure beyond the band of critical frequencies.

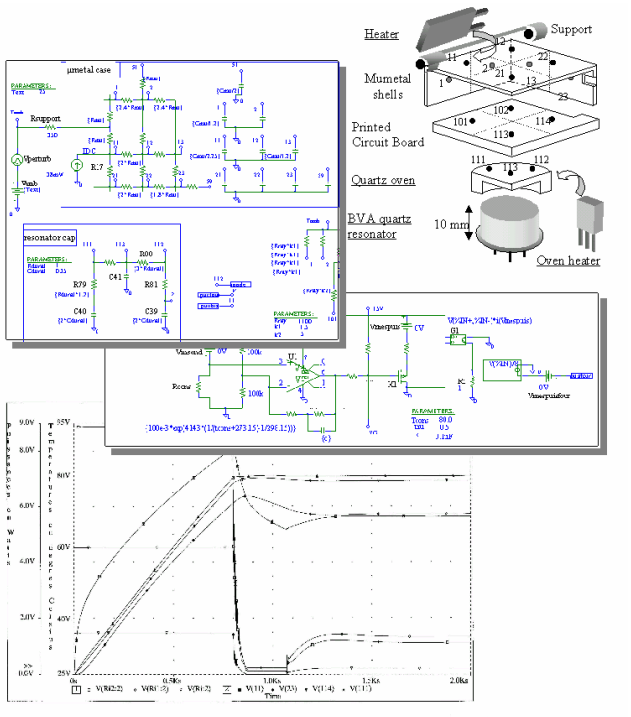

Fig. 4. The structure is manually meshed and described by an electrical network. Then the thermal control loop can easily be closed with its electrical part and the control system operates. Resulting data are voltages for temperatures and currents for heat flows in the electrical analogy.

Although finite element methods are very efficient to provide the resulting temperature map for given boundary conditions in terms of heat flow and temperature, they cannot include the closed-loop control system. The analysis of the temperature distribution and its associated temperature control has been performed with the electrical analogy [4][5]. This is illustrated in Fig. 4.

The heart of the oscillator is precisely temperature-controlled and its thermal regulator also acts on external heater glued on mumetal shells. In such a way the resonator in its oven is the best temperature-controlled part as well as the oscillator electronics. The inner temperature is typically 82 °C. Temperature of mumetal shells is then between the inner an external temperatures and slightly fluctuates versus the external one because their heaters are just actuated from the inner regulator. The mean mumetal shells temperature is typically 10°C below the oven temperature.

IV. Experimental results

A. Thermal sensitivity

Obviously, frequency sensitivity versus ambient temperature depends on the adjustment of the set temperature. This is illustrated in Fig. 5 when the oscillator is working at atmospheric pressure and under vacuum. In the latter case, the experiment length is about 50 hours. This is why aging has been removed. In this example the set temperature is probably a little bit above the resonator turn over temperature.

One can observe that under vacuum the thermal sensitivity is lower than at atmospheric pressure. Nevertheless, radiative exchanges can be estimated to be 30 % of the overall thermal losses.

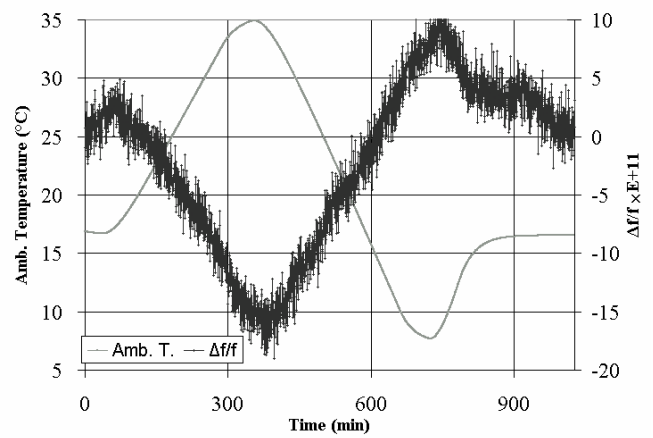

(a)

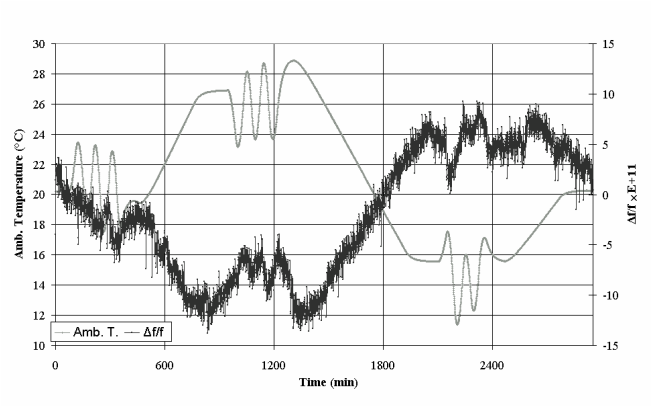

(b)

Fig. 5. Relative frequency change versus ambient temperature (a) at atmospheric pressure (b) under vacuum

As an example, in Fig. 6 the set temperature is optimal. The frequency-temperature sensitivity is quite invisible. Residual change is essentially due to aging (typically 2 10^{-10} per day)

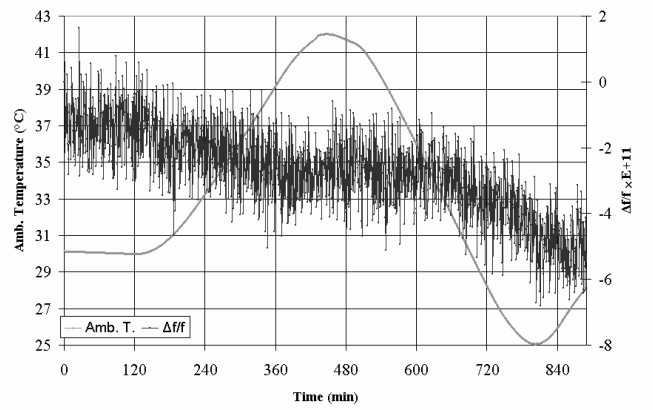

Fig. 6. An example of an optimal adjustment of set temperature.

B. Behavior under vibrations

Because this oscillator is designed to work in a satellite, it must also endure the launch of the spacecraft used for the transportation. During the launch it is submitted to vibrations. So this type of test is necessary. To do that, all parts of Fig. 1 are glued before sealing the oscillator enclosure. Test of vibrations is performed according to the axis system of Fig. 1-a. The oscillator is submitted to a random noise whose power spectral density is 0.05 g^2/Hz. Results are shown in Fig. 7. On each axis vibrations are turned on at mark **1**. Power is increasing from mark **2**, reaches its nominal value at mark **3** and is maintained at this value up to mark **4**. Note that when the oscillator is turned upside down from one axis to the following axis, a frequency step is recorded.

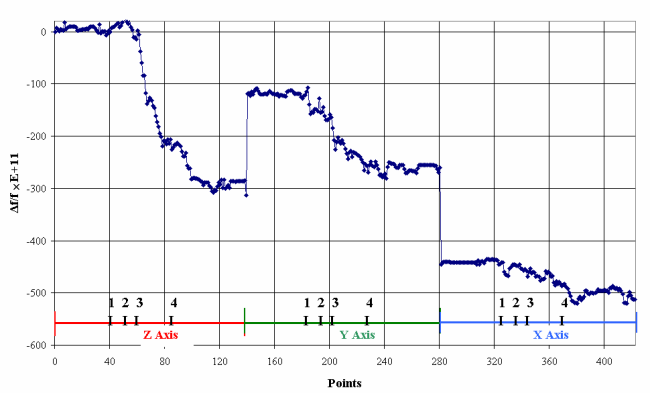

Fig. 7. Vibrations test with a random noise whose power spectral density is 0.05 g^2/Hz

C. Magnetic sensitivity

Fig. 8 demonstrates the efficiency of the mumetal shells. It shows records of the frequency change when a magnetic field of ± 6 Gauss is applied along one of the three axis of the oscillator (see Fig. 1-a for the axis sytem) with and without mumetal shells. When mumetal shells are used the oscillator becomes completely insensitive to this magnetic field.

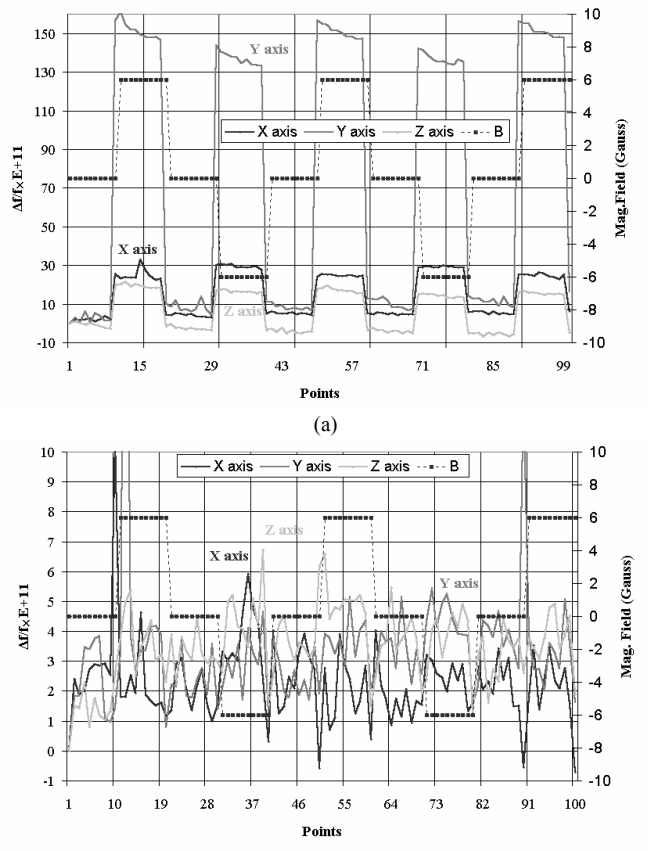

Fig. 8. Effect of a magnetic field of ± 6 Gauss (a) without mumetal shells (b) with mumetal shells.

D. Frequency stability

Fig. 9 shows a typical one-sided power spectral density of phase fluctuations of an oscillator equipped with a resonator taken from a recent BVA resonator batch. Results are quite poor. We would expect better result close to the carrier, that is to say at least –120 dBc/Hz at 1Hz from the carrier. Indeed, the oscillator electronic here used coupled with BVA resonators coming from older crystal batches has already exhibited very good results before ($\sigma(\tau) = 5\ 10^{-14}$ for 1 s < τ < 5 s). Although these good resonators were sorted out [6], unfortunately such an operation does not give the same result with recent batches. The experimental Allan variance of oscillators equipped with various samples of recently manufactured resonators is detailed in table 1. Otherwise, noise measurements of these resonators (whose $\mathcal{L}(f = 1\ Hz)$ is not better than -135dBc/Hz, measured with a passive method) confirmed that there is no excellent unit in these batches.

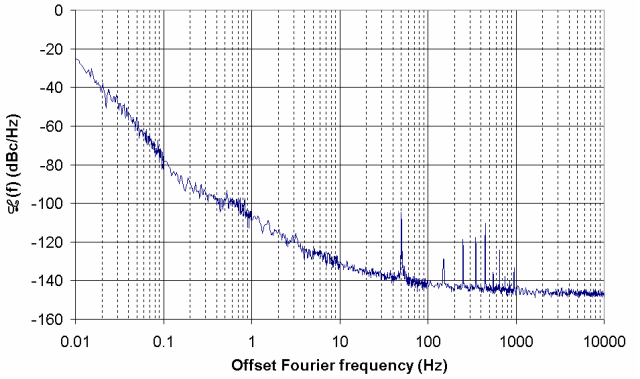

Fig. 9. Typical one-sided power spectral density of phase fluctuations.

TABLE I
Measured Allan variances of oscillators equipped with recent resonators

τ (s)	0.5	1	2	4	6	8	10
$\sigma_y(\tau)$ (10^{-13}) # 5103	7.3	4.6	1.75	2.7	3.2	3.35	3.45
$\sigma_y(\tau)$ (10^{-13}) # 5510	2.5	1.9	1.9	1.8	1.8	1.9	1.95
$\sigma_y(\tau)$ (10^{-13}) # 5614	5.6	1.8	1.8	2.25	2.9	3.5	3.9
$\sigma_y(\tau)$ (10^{-13}) # 5613	3.9	3.6	5.14	8.9	11	12	14

V. Conclusion

When submitted to various disturbances of its environment, this new oscillator design exhibits results in accordance with the intended behavior. Unfortunately, the observed frequency stabilities are disappointing and verified from noise measurements performed on couples of resonators taken from recent BVA resonator batches. Actually, it seems that the only way to get good resonator units is selection, which is difficult for a weak laboratory production. It is obvious that the solution would be to relate the resulting resonator noise to operations of the manufacture process

ACKNOWLEDGEMENTS

The authors thank X. Penou, N. Franquet and P. Cassard for their help in the project achievement.

REFERENCES

[1] R. J. Besson, M. Mourey, S. Galliou, F. Marionnet (ENSMM France), F. Gonzalez, P. Guillemot (CNES France), R. Tjoelker, W. Diener, A. Kirk (JPL USA), "10 MHz Hyperstable Quartz Oscillators Performances", *joint meeting of the 13th European Fequency and Time Forum and 1999 IEEE International Frequency Control Symposium*, Besançon France, pp 326-330, vol.1, May 1999.

[2] S. Galliou, F. Sthal, M. Mourey, "Enhanced phase noise model for quartz crystal oscillators," Proc. 56th IEEE Ann. Freq. Cont. Symp., New Orleans, Louisiana, 29-31 May, pp. 627-632, (2002).

[3] S. Galliou, F. Sthal, N. Gufflet, M. Mourey, "Predicting phase noise in crystal oscillators," In these proceedings.

[4] S. Galliou, M. Mourey, "Temperature processing of an ultra stable quartz oscillator", *IEEE transactions on Ultrasonics, Ferroelectrics, and Frequency Control*, vol. 48, no 6, pp 1539-1546, 2001.

[5] B. Hillerich, O. Nagler, " Application of finite element method and SPICE simulations for design optimisation of oven-controlled crystal oscillator" *IEEE transactions on Ultrasonics, Ferroelectrics, and Frequency Control*, vol. 48, no 6, pp 1662-1668, 2001.

[6] F. Sthal, M. Mourey, F. Marionnet and W. F. Walls, "Phase noise measurements of 10-MHz BVA quartz crystal resonators," *IEEE Trans. Ultrason., Ferroelect., Freq. Contr., vol. 47*, no. 2, pp. 369-373, Mar. 2000.